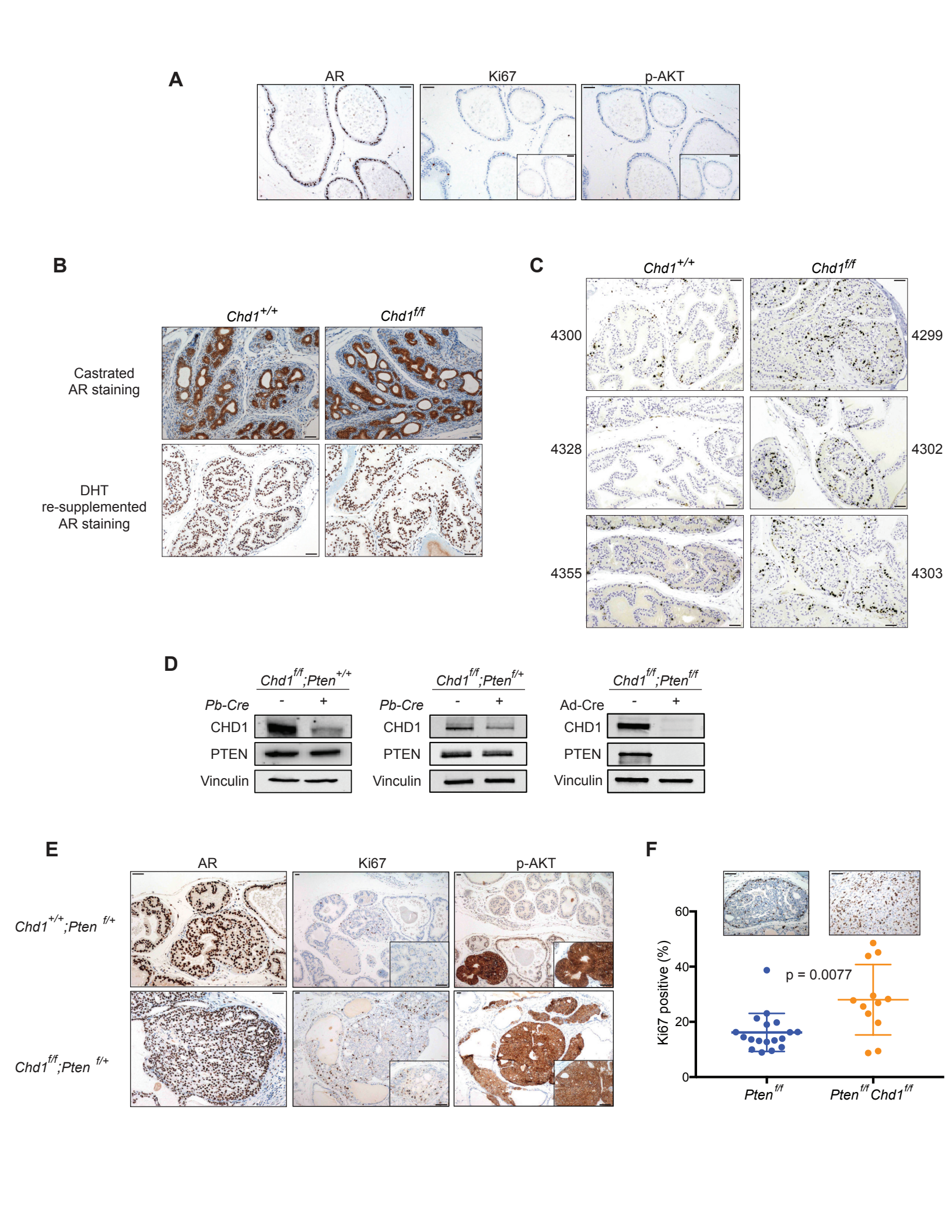
A
AR
Ki67
p-AKT
B
Chd1+/+
Chd1f/f
Castrated
AR staining
DHT
re-supplemented
AR staining
C
Chd1+/+
Chd1f/f
4300
4299
4328
4302
4355
4303
D
Chd1f/f;Pten+/+
Chd1f/f;Ptenf/+
Chd1f/f;Ptenf/f
Pb-Cre
Ad-Cre
CHD1
PTEN
Vinculin
E
AR
Ki67
p-AKT
Chd1+/+;Pten f/+
Chd1f/f;Pten f/+
F
Ki67 positive (%)
60
40
20
0
p = 0.0077
Pten f/f
Pten f/f Chd1 f/f

Figure S1. *Chd1* loss exacerbates neoplastic phenotypes *in vivo.* Related to Figure 1.

(A) Representative images of immunostaining from 1 year old *Chd1$^{f/f}$;Pb-Cre^{+}* prostates stained for AR, Ki67, and p-AKT. Scale bar 50 μm.

(B) Immunohistochemical staining for AR in murine prostates after castration (top-cytoplasmic staining) or castration-androgen re-supplementation (bottom-nuclear staining). Scale bar 50 μm.

(C) Staining of murine prostates for Ki67 2 weeks post testosterone re-supplementation. 3 independent *Chd1$^{+/+}$* and *Chd1$^{f/f}$* mice are shown (n = 4 *Chd1$^{+/+}$* and n = 6 *Chd1$^{f/f}$)*. Adjacent numbers are in-house identifiers of individual mice. Scale bar 50 μm.

(D) Immunoblots of murine prostates of the given genotype.

(E) Immunohistochemistry for AR, Ki67, and p-AKT from 1 year old prostates of the given genotype. Scale bar 50 μm.

(F) Quantification of Ki67 from *Chd1$^{+/+}$;Pten$^{f/f}$;Pb-Cre^{+}* and *Chd1$^{f/f}$;Pten$^{f/f}$*; *Pb-Cre^{+}* mice at 1 year of age. Comparison utilized a student's t-test. Scale bar 50 μm. Data represents +/- SEM.

A

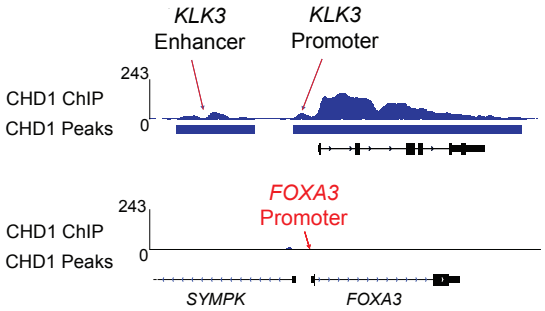
KLK3
Enhancer
KLK3
Promoter
243
CHD1 ChIP
CHD1 Peaks
0
FOXA3
Promoter
243
CHD1 ChIP
CHD1 Peaks
0
SYMPK
FOXA3

B

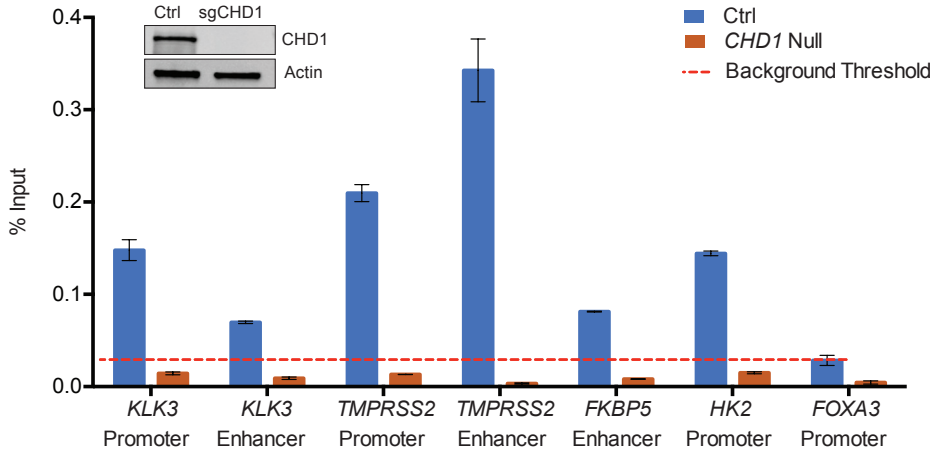
Ctrl
sgCHD1
CHD1
Actin
Ctrl
CHD1 Null
Background Threshold
% Input
0.4
0.3
0.2
0.1
0.0
KLK3 Promoter
KLK3 Enhancer
TMPRSS2 Promoter
TMPRSS2 Enhancer
FKBP5 Enhancer
HK2 Promoter
FOXA3 Promoter

Figure S2. **Genome-wide binding of CHD1 is specific to CHD1 expressing cells. Related to Figure 2.**

(A) Snapshot of CHD1 ChIP Seq signal at the *KLK3* locus (positive for binding) and *FOXA3* promoter (negative for binding).

(B) LNCaP cells CRISPR engineered to eliminate expression of CHD1 (inset immunoblot), were assessed for background CHD1 ChIP signal under androgen proficient conditions at several positive and negative CHD1 loci (determined by ChIP Seq) by qPCR. The *FOXA3* promoter serves as a negative background control signal (indicated by horizontal red dotted line). Data represents +/- SEM.

A

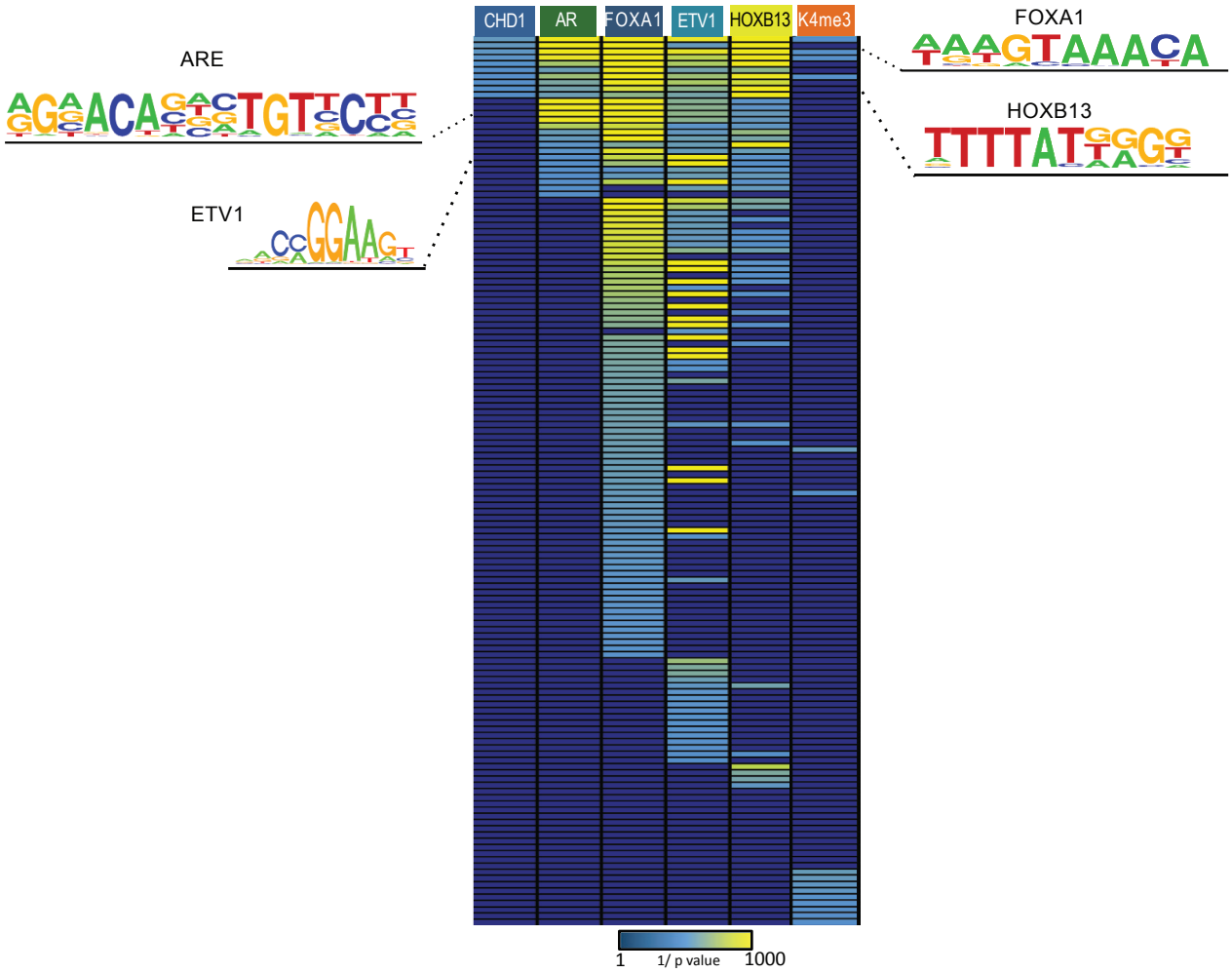
CHD1
AR
FOXA1
ETV1
HOXB13
K4me3
ARE
ETV1
FOXA1
HOXB13
1
1/ p value
1000

Figure S3. **Genome-wide binding of CHD1 is not significantly associated with any one motif. Related to Figure 4.**

(A) ChIP sequencing peaks for CHD1, AR, H3K4me3, HOXB13 (Pomerantz et al., 2015), ETV1 (Chen et al., 2013), and FOXA1 (Zhao et al., 2016), were analyzed for motif enrichment within a 200 bp window around the peak center. All Jasper motifs with a p value less than 0.01 are plotted for each factor.

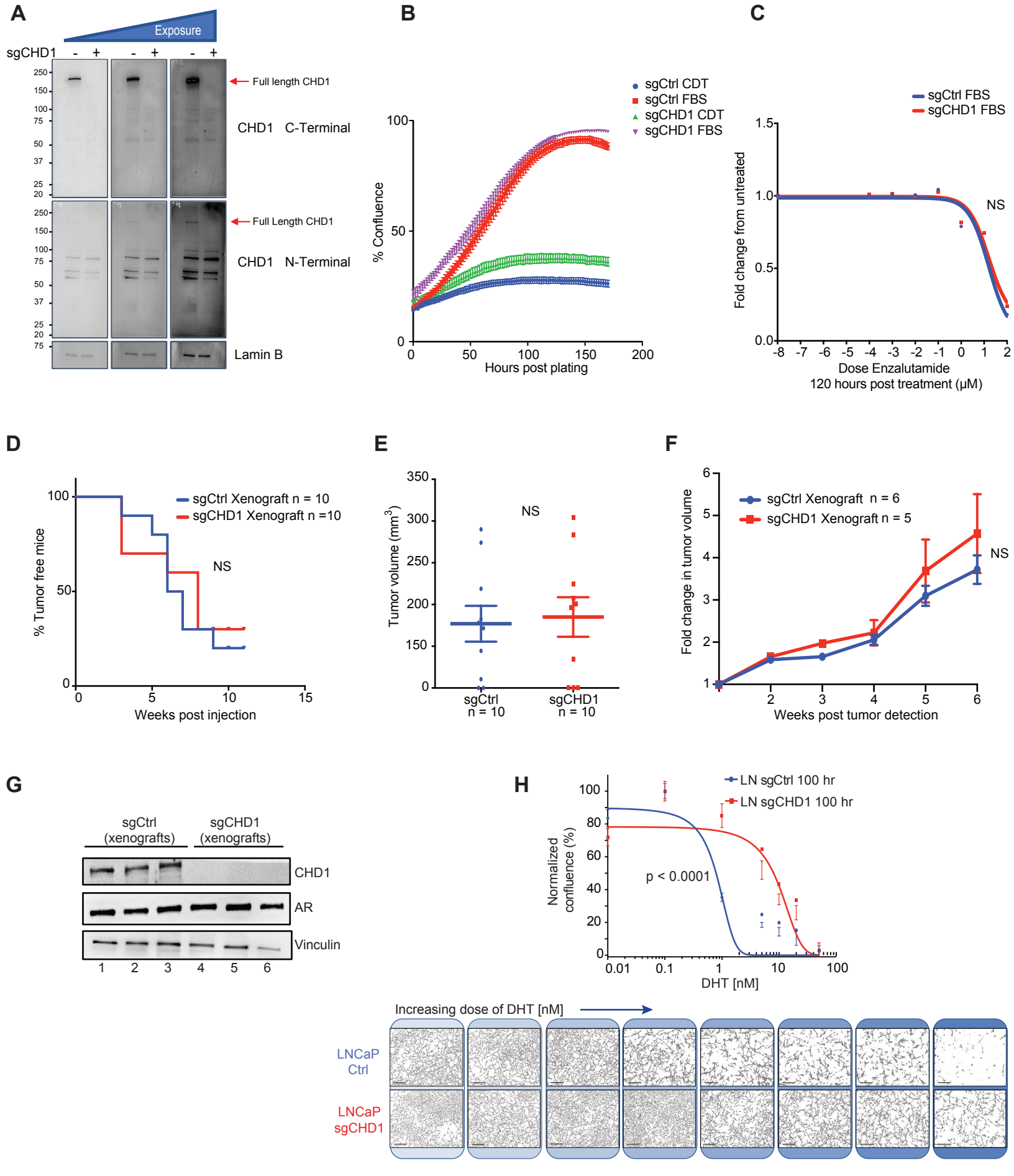
A
Exposure
sgCHD1 - + - + - +
250
150
100
75
50
37
25
20
Full length CHD1
CHD1 C-Terminal
Full Length CHD1
CHD1 N-Terminal
Lamin B
B
sgCtrl CDT
sgCtrl FBS
sgCHD1 CDT
sgCHD1 FBS
% Confluence
Hours post plating
C
sgCtrl FBS
sgCHD1 FBS
Fold change from untreated
NS
Dose Enzalutamide
120 hours post treatment (μM)
D
sgCtrl Xenograft n = 10
sgCHD1 Xenograft n =10
% Tumor free mice
NS
Weeks post injection
E
Tumor volume (mm3)
NS
sgCtrl
n = 10
sgCHD1
n = 10
F
sgCtrl Xenograft n = 6
sgCHD1 Xenograft n = 5
Fold change in tumor volume
NS
Weeks post tumor detection
G
sgCtrl
(xenografts)
sgCHD1
(xenografts)
CHD1
AR
Vinculin
1 2 3 4 5 6
H
LN sgCtrl 100 hr
LN sgCHD1 100 hr
Normalized confluence (%)
p < 0.0001
DHT [nM]
Increasing dose of DHT [nM]
LNCaP Ctrl
LNCaP sgCHD1

Figure S4. Models of *CHD1* genomic loss of are sensitive to androgen status and show no defects in growth or tumorigenicity *in vivo*. Related to Figure 5.

(**A)** LNCaP cells stably expressing sgCtrl or sgCHD1 guide RNAs were assessed for CHD1 expression using antibodies directed against the N or C terminus of human CHD1. Full gels are shown for each antibody with increasing exposure images shown from left to right.

(B) Models from A were grown in androgen proficient (FBS) or androgen deficient (Charcoal Dextran Treated-FBS) conditions and growth (confluency) was measured over time.

(C) Models from A were treated with increasing doses of Enzalutamide and growth (Incucyte-confluency) measured over time. Fold change in confluency from vehicle was calculated for each dose. Non-linear regression was used to define IC_{50} values.

(D) Models from A were injected into the flanks of athymic male mice (6-8 weeks of age) and monitored for tumor growth over time.

(E) Volume of all tumors injected 10 weeks post injection (mm^3).

(F) Tumor volume for each line is plotted as a function of initial volume at the time of detection.

(**G)** Individual tumors were harvested from mice and grown as 3D organoids in matrigel. After 3 passages, each individual tumor-organoid was assessed for CHD1 and AR status via immunoblot.

(**H**) Dose response curve of each cell line in response to DHT, calculated as in C (top) and, representative images of each cell line at each dose of androgen 96 hours post plating (bottom). Scale bar 20 μm.

For all panels in this figure, data represents +/- SEM. NS - not significant.

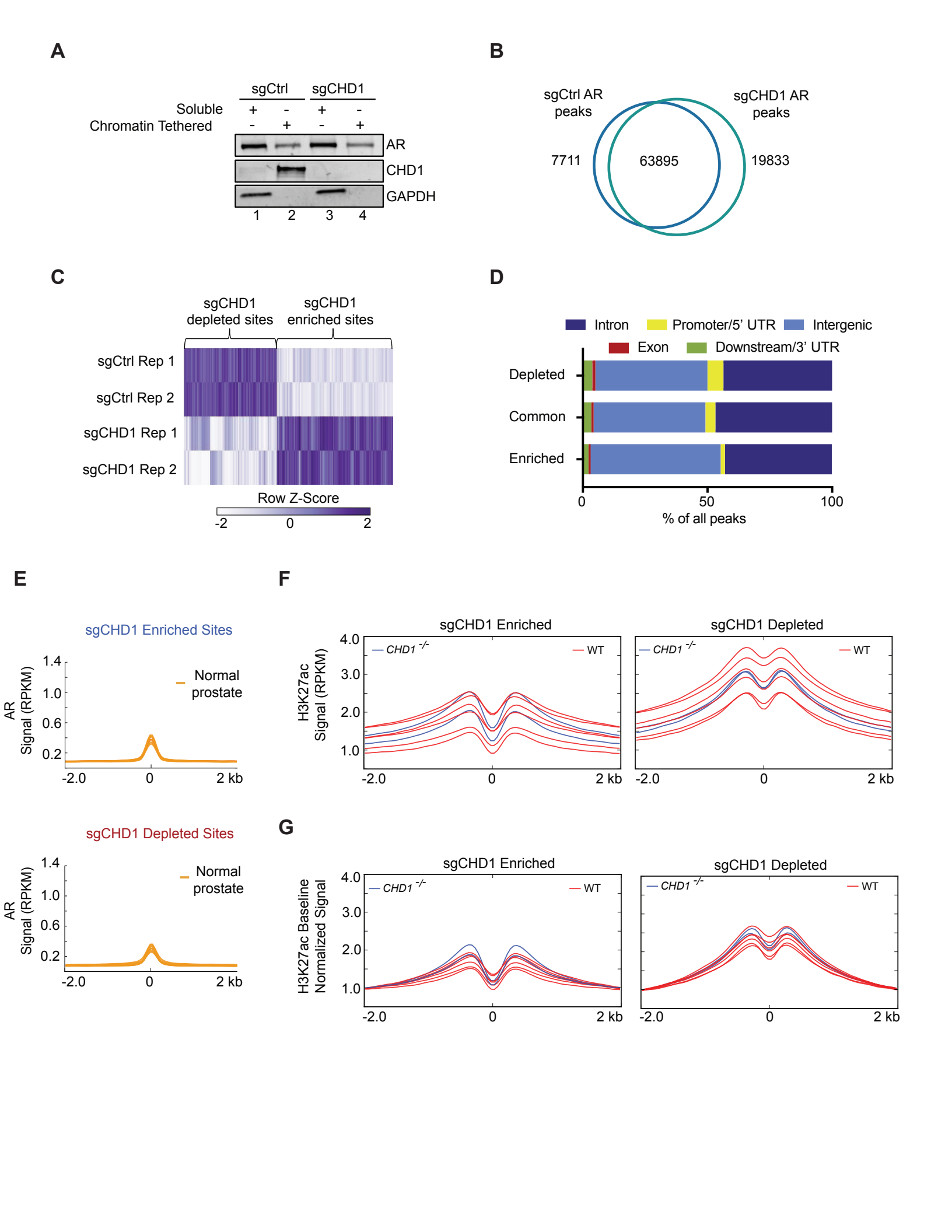
A
sgCtrl
sgCHD1
Soluble
Chromatin Tethered
+ - + -
- + - +
AR
CHD1
GAPDH
1 2 3 4
B
sgCtrl AR peaks
sgCHD1 AR peaks
7711
63895
19833
C
sgCHD1 depleted sites
sgCHD1 enriched sites
sgCtrl Rep 1
sgCtrl Rep 2
sgCHD1 Rep 1
sgCHD1 Rep 2
Row Z-Score
-2 0 2
D
Intron
Promoter/5' UTR
Intergenic
Exon
Downstream/3' UTR
Depleted
Common
Enriched
0 50 100
% of all peaks
E
sgCHD1 Enriched Sites
AR Signal (RPKM)
1.4 1.0 0.6 0.2
Normal prostate
-2.0 0 2 kb
sgCHD1 Depleted Sites
AR Signal (RPKM)
1.4 1.0 0.6 0.2
Normal prostate
-2.0 0 2 kb
F
sgCHD1 Enriched
sgCHD1 Depleted
H3K27ac Signal (RPKM)
4.0 3.0 2.0 1.0
CHD1 -/-
WT
-2.0 0 2 kb
G
sgCHD1 Enriched
sgCHD1 Depleted
H3K27ac Baseline Normalized Signal
4.0 3.0 2.0 1.0
CHD1 -/-
WT
-2.0 0 2 kb

Figure S5. *CHD1* loss redistributes AR to subclass-enriched enhancer sites. Related to Figure 5.

(A) Chromatin tethering of AR and CHD1 in sgCtrl and sgCHD1 cell in the presence of androgen (similar to ChIP seq conditions). GAPDH serves as a soluble specific control.

(B) Peak overlap for AR in Ctrl and sgCHD1 LNCaP cells. Peaks were called using MACS2 and q of 0.05. The overlap window was set at a minimum of 1 bp.

(C) Heatmap of individual replicate z-score for differentially bound peaks between sgCtrl and sgCHD1 cells, determined using the DiffBind R package (FDR = 0.01).

(D) CEAS analysis of differentially bound and common peaks identified in C.

(E) AR ChIP seq from normal prostate tissue (n = 7) (GSE70079-(Pomerantz et al., 2015)) was assessed for enrichment at sgCHD1 enriched and depleted sites.

(F) H3K27ac ChIP sequencing derived from primary human prostate tumors (GSE96652-(Kron et al., 2017)) was analyzed for signal pileup at sgCHD1 enriched and depleted sites and annotated for *CHD1* genomic status (*CHD1* null-blue and *CHD1* WT-red) utilizing the published bigwig files.

(G) The baseline signal for each individual tumor from F was normalized to 1 and plotted at sgCHD1 enriched and depleted sites.

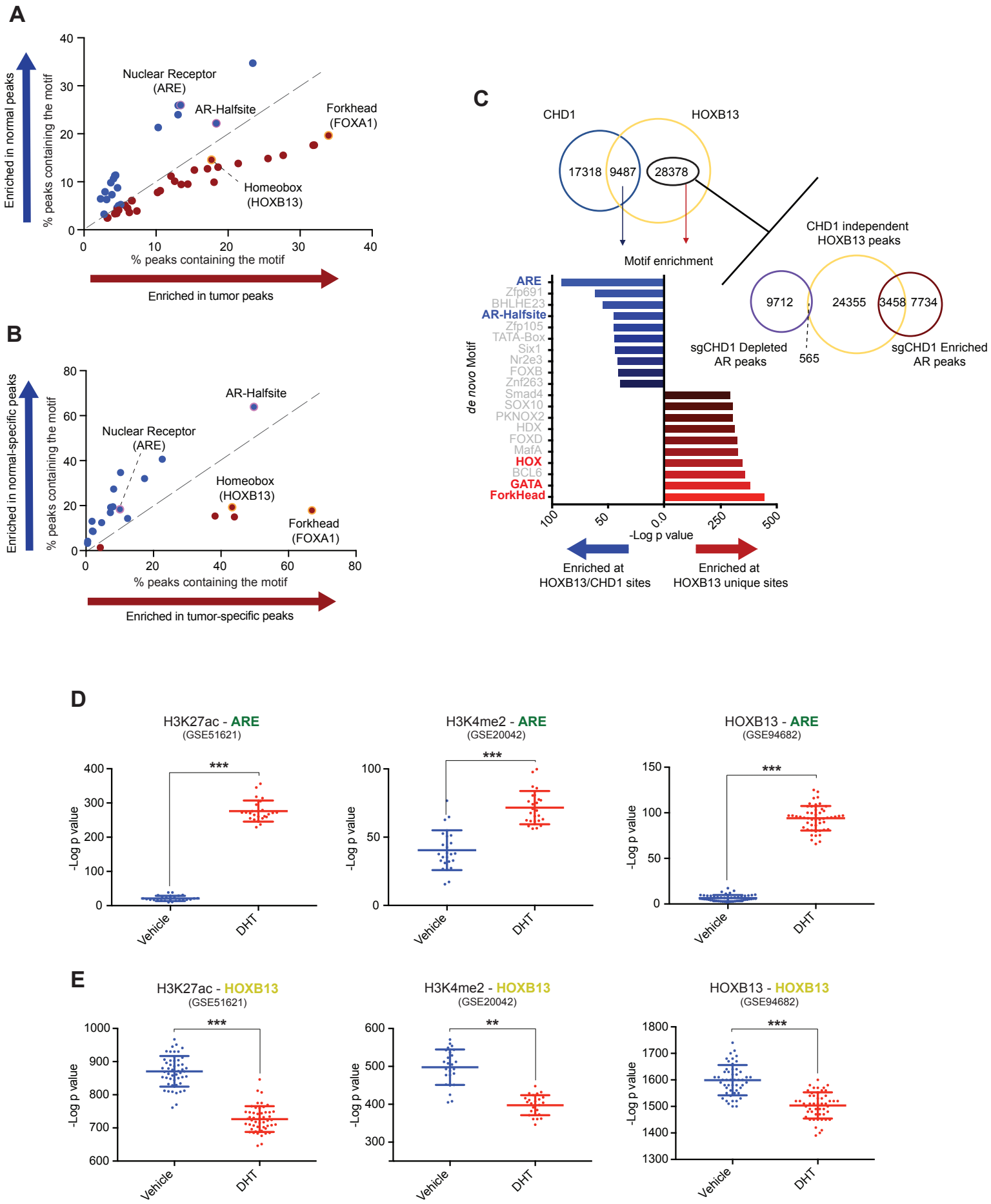
A
Enriched in normal peaks
% peaks containing the motif
Nuclear Receptor (ARE)
AR-Halfsite
Forkhead (FOXA1)
Homeobox (HOXB13)
% peaks containing the motif
Enriched in tumor peaks
B
Enriched in normal-specific peaks
% peaks containing the motif
AR-Halfsite
Nuclear Receptor (ARE)
Homeobox (HOXB13)
Forkhead (FOXA1)
% peaks containing the motif
Enriched in tumor-specific peaks
C
CHD1
HOXB13
17318
9487
28378
Motif enrichment
de novo Motif
ARE
Zfp691
BHLHE23
AR-Halfsite
Zfp105
TATA-Box
Six1
Nr2e3
FOXB
Znf263
Smad4
SOX10
PKNOX2
HDX
FOXD
MafA
HOX
BCL6
GATA
ForkHead
-Log p value
Enriched at HOXB13/CHD1 sites
Enriched at HOXB13 unique sites
CHD1 independent HOXB13 peaks
9712
24355
3458
7734
565
sgCHD1 Depleted AR peaks
sgCHD1 Enriched AR peaks
D
H3K27ac - ARE
(GSE51621)
H3K4me2 - ARE
(GSE20042)
HOXB13 - ARE
(GSE94682)
-Log p value
Vehicle
DHT
E
H3K27ac - HOXB13
(GSE51621)
H3K4me2 - HOXB13
(GSE20042)
HOXB13 - HOXB13
(GSE94682)
-Log p value
Vehicle
DHT

Figure S6. The CHD1 null AR cistrome is enriched for CHD1 independent HOX motifs . Related to Figure 6.

(A) Peaks derived from AR ChIP seq from normal (n = 7) and primary PCa (n = 13) (GSE70079- (Pomerantz et al., 2015)) were merged and assessed for motif enrichment around the center of each peak using Homer v3. The % of peaks (background subtracted) containing significantly enriched motifs ($p < 10^{-20}$) is plotted for both normal and tumor samples. The dotted line separates normal (blue) from tumor (red) enrichment.

(B) Motif analysis reported in (Pomerantz et al., 2015) of peaks uniquely enriched in either normal or tumor tissue, is plotted as in A and demonstrates an enrichment of HOX and FOX motifs and depletion of AR Half-site motifs in the PCa-specific AR cistrome.

(C) The overlap between the CHD1 and HOXB13 ((Pomerantz et al., 2015) cistromes in LNCaP cells is reported (top) and motif enrichment for common (blue) or CHD1 independent HOXB13 peaks (red) was performed using the opposing dataset as background. The top 10 *de novo* motifs are shown for each peak set (bottom). The overlap between the CHD1 independent HOXB13 cistrome and AR enriched and depleted peaks in sgCHD1 cells (right).

(D) LNCaP cells deprived of testosterone and then treated with vehicle or androgen were assessed for the ARE motif at H3K4me2 (GSE20042 - (He et al., 2010)), H3K27ac (GSE51621 - (Hazelett et al., 2014)), and HOXB13 (GSE94682 - (Stelloo et al., 2018)) ChIP Seq peaks. Pre-called peaks were randomly sampled 25x for ARE enrichment, and the mean of each condition is reported. 2 tailed students t-test; ** $p < 0.005$, *** $p < 0.0001$. Data represents +/- SEM.

(E) Enrichment of the HOXB13 motif was assessed for each condition as in D. 2 tailed students t-test; ** $p < 0.005$, *** $p < 0.0001$. Data represents +/- SEM.

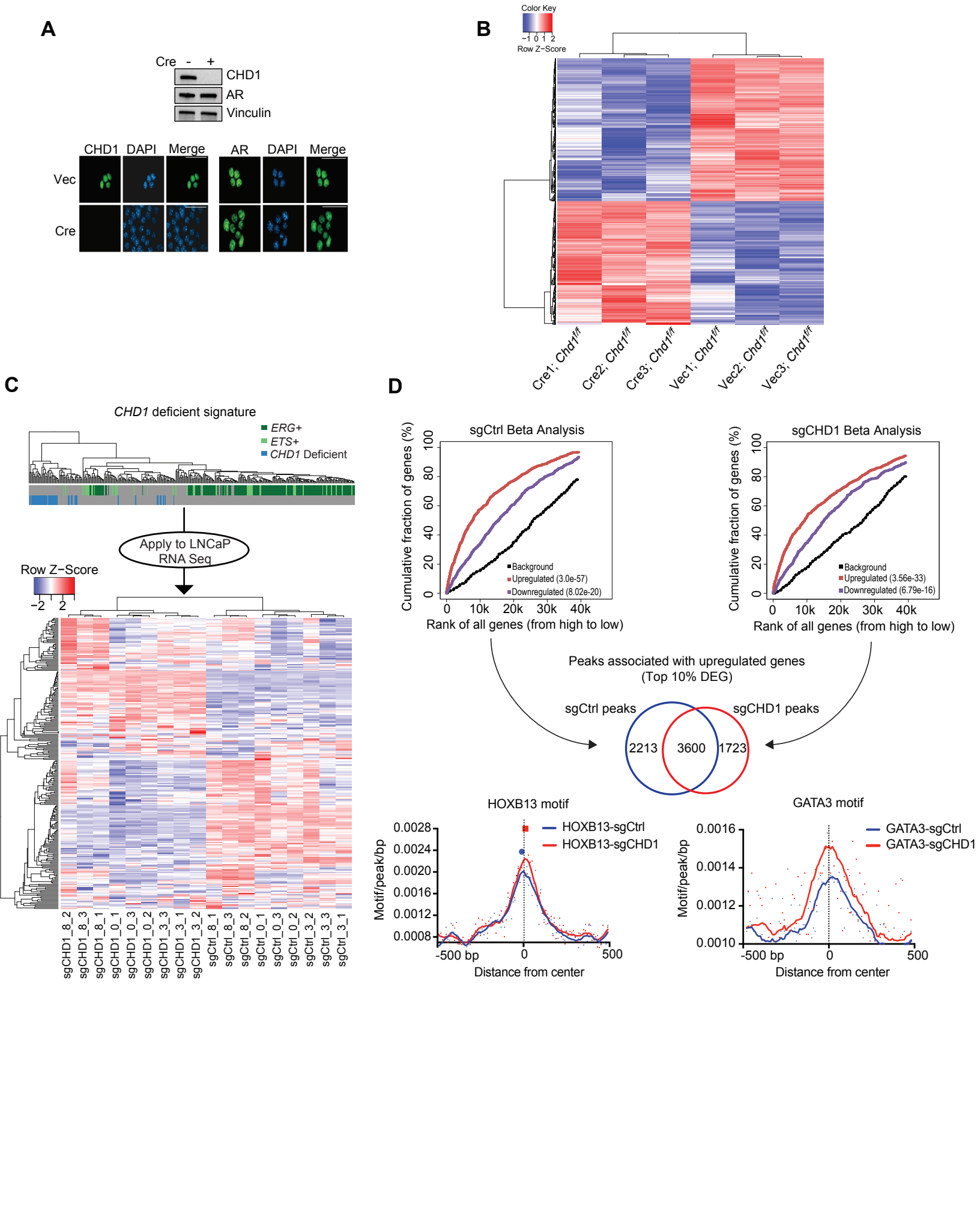
A
Cre - +
CHD1
AR
Vinculin
CHD1 DAPI Merge
AR DAPI Merge
Vec
Cre
B
Color Key
−1 0 1 2
Row Z−Score
Cre1; Chd1f/f
Cre2; Chd1f/f
Cre3; Chd1f/f
Vec1; Chd1f/f
Vec2; Chd1f/f
Vec3; Chd1f/f
C
CHD1 deficient signature
ERG+
ETS+
CHD1 Deficient
Apply to LNCaP RNA Seq
Row Z−Score
−2 2
sgCHD1_8_2
sgCHD1_8_3
sgCHD1_8_1
sgCHD1_0_1
sgCHD1_0_3
sgCHD1_0_2
sgCHD1_3_3
sgCHD1_3_1
sgCHD1_3_2
sgCtrl_8_1
sgCtrl_8_3
sgCtrl_8_2
sgCtrl_0_1
sgCtrl_0_3
sgCtrl_0_2
sgCtrl_3_2
sgCtrl_3_3
sgCtrl_3_1
D
sgCtrl Beta Analysis
Cumulative fraction of genes (%)
Rank of all genes (from high to low)
Background
Upregulated (3.0e-57)
Downregulated (8.02e-20)
sgCHD1 Beta Analysis
Background
Upregulated (3.56e-33)
Downregulated (6.79e-16)
Peaks associated with upregulated genes
(Top 10% DEG)
sgCtrl peaks
sgCHD1 peaks
2213
3600
1723
HOXB13 motif
HOXB13-sgCtrl
HOXB13-sgCHD1
Motif/peak/bp
Distance from center
GATA3 motif
GATA3-sgCtrl
GATA3-sgCHD1

Figure S7. Prostate derived models of *CHD1* loss display unique patterns of transcriptional regulation. Related to Figure 7.

(A) Organoids were derived from the prostate of a 3-month-old male mouse with homozygously floxed *Chd1* alleles, grown for 2 passages, then treated with either vector or Cre expressing Adeno-virus for 12 hours. 96 hours post infection, cells were harvested for immunoblotting to validate *Chd1* deletion and AR positivity (top). Organoids were stained for CHD1 and AR via immunofluorescence to confirm a homogenous population of CHD1 null and AR positive cells (bottom). Scale bar 20 μm.

(B) Heatmap of significantly differentially expressed genes (RNA-Seq) in cells derived from A.

(C) Clustering of primary PCa samples (TCGA) based upon a *CHD1* null tumor signature derived from TCGA data (top) and clustering the isogenic model of *CHD1* loss in LNCaPs (RNA-seq 0, 3, and 8 hours of DHT) based upon the *CHD1* null signature above (bottom).

(D) Beta analysis of isogenic LNCaP model of *CHD1* loss utilizing the identified AR cistrome (all peaks) and transcriptional changes (RNA-seq at 0 vs 8 hours 1 nM DHT) in each cell model. Peaks were identified for the top 10% of the differentially expressed genes for each model and motif density for each peak set determined for HOXB13 and GATA3.

Table S5: Detailed primer list, related to STAR Methods.

Name	Sequence 5'--->3'	Ref
KLK3 enhancer F	TGGGACAACTTGCAAACCTG	Shang et al., 2002 Mol Cell
KLK3 enhancer R	CCAGAGTAGGTCTGTTTTCAATCCA	
TMPRSS2 ARE V F	TGGTCCTGGATGATAAAAAAAGTTT	Wang et al., 2007 Mol Cell
TMPRSS2 ARE V R	GACATACGCCCCACAACAGA	
FOXA3 Promoter F	ATGGGGATGTGATTTCGGGG	This paper
FOXA3 Promoter R	AATCAGAACGCTAGGGCCAC	
KLK3 promoter F	CCTAGATGAAGTCTCCATGAGCTACA	Shang et al., 2002 Mol Cell
KLK3 promoter R	GGGAGGGAGAGCTAGCACTTG	
FKBP5 ARE 6/7 F	CCCCCCTATTTTAATCGGAGTAC	Magee et al., 2006 Endocrinology
FKBP5 ARE 6/7 R	TTTTGAAGAGCACAGAACACCCT	
HK2 Promoter F	CTTCTGCAGCGCGAGTTC	Anderson et al., 2012 JCI
HK2 Promoter R	GAACCGCTCGTCTCCTACAC	
Chd1 genotyping F	AGAGGACAGCGTGACTAAAGC	This paper
Chd1 genotyping R	CATTCCATCAAACAATTAGAACCACATCTT	
Pten WT F	ATTAAACTGCTTGACAGCACAGC	Wu et al., 2001
Pten WT R	AGAAAGCTCTTCACTGCACACA	
Pten floxed F	CTTGACAGCACAGCGTTGT	Wu et al., 2001
Pten floxed R	TGTATGCTATACGAAGTTATTAGGTCCCT	

Table S6: Detailed antibody usage, related to STAR Methods.

Name	Company	Application	Dilution	Cat #
Alexa Fluor 488 Goat anti-mouse	Invitrogen	IF	1:500	A-11029
Alexa Fluor 555 Goat anti-rabbit	Invitrogen	IF	1:500	A-21428
alpha-Tubulin	Cell Signaling	Immunoblot	1:1000	2144S
Androgen Receptor	Abcam	IHC	1:500	ab108341
Androgen Receptor	Abcam	ChIP	4 µg	ab74272
Androgen Receptor	Abcam	PLA	1:500	ab9474
Androgen Receptor	Santa Cruz	ChIP/Immunoblot/IF	4 µg/1:1000/1:500	sc-816 X
anti-goat HRP	Thermo Fisher	Immunoblot	1:5000	31402
anti-rabbit HRP	Pierce	Immunoblot	1:5000	32260
c-MYC	Santa Cruz	ChIP	8 µg	sc-764 X
CHD1	Bethyl	ChIP	10 µg	A301-218A
CHD1	Cell Signaling	IF/PLA/Immunoblot	1:50/1:50/1:1000	4351S
H3K27me3	Abcam	ChIP	2 µg	ab195477
H3K4me2	Abcam	ChIP	2 µg	ab7766
H3K4me3	Abcam	ChIP	2 µg	ab8580
HOXB13	Santa Cruz	Immunoblot	1:1000	sc-66923
Lamin B	Santa Cruz	Immunoblot	1:1000	sc-6217
Mouse IgG	BioLegend	RIME	4 µg	400102
Rabbit IgG	Abcam	RIME	4 µg	ab37415
Vinculin	Abcam	Immunoblot	1:1000	ab129002
Beta-actin	Invitrogen	Immunoblot	1:1000	PIMA515739
mKi67	Abcam	IHC	1:200	ab16667
CHD1	Active Motif	Immunoblot	1:500	39730